XII. SIGNAL PROCESSING

Academic and Research Staff

Prof. A. G. Bose
Prof. J. D. Bruce
Prof. D. E. Nelsen
Prof. A. V. Oppenheim
Prof. C. L. Searle
Prof. H. J. Zimmermann
Dr. M. V. Cerrillo

Graduate Students

J. B. Bourne
M. Bruce-Lockhart
M. F. Davis
D. A. Feldman
R. M. Mersereau
T. L. Rhyne
J. R. Samson, Jr.
L. M. Sivertson
R. E. Stewart

A. OPTIMAL LINEAR FILTER FOR ESTIMATION OF GROUP TIME OF ARRIVAL

The problem of optimal linear filtering of Loran C pulsed radio transmissions is being studied. Two related linear time-invariant filter operations were considered for estimating phase time of arrival and group time of arrival. The filter operations described in this report will be applied to the signal in place of the bandpass "RF" filters of a Loran C radio navigation receiver. Optimality was considered in the sense of maximizing the ratio(s) of desired signal parameter(s)-to-noise variance ratio at the output of the filter(s), in response to the Loran C pulse and an uncorrelated shaped noise spectrum. For phase time of arrival the signal parameter of interest was that of a maximum signal envelope at a specified sample time. For group time of arrival the resulting signal was constrained to have a zero crossing at the specified sample time, while the signal parameter of interest was that of the signal slope at the zero crossing.

In the Loran C context the optimal filter for estimating phase time of arrival is the familiar "matched-filter" result stated in the Wiener-Hopf equation (Eq. 1). The optimal filter for Loran C group arrival time is the more general result stated in Eq. 2, which gives the optimal linear filter for maximizing the ratio of slope-to-noise standard deviation of a filter, thereby causing a response passing through zero at time "T". The filter transforms $H_p(s)$ and $H_g(s)$ are specified by the pulse spectrum P(s), the factored noise-power spectrum $\phi^+(s)$ and $\phi^-(s)$, the sample time T, and the given constant C.

$$\underline{h_p(t)} \longleftrightarrow H_p(s) = \frac{1}{\phi^+(s)} \left[\text{causal} \left(\frac{P(-s)\, e^{-sT}}{\phi^-(s)} \right) \right]. \tag{1}$$

---

*This work is supported by the Joint Services Electronics Programs (U.S. Army, U.S. Navy, and U.S. Air Force) under Contract DA 28-043-AMC-02536(E).

$$\underline{h_g(t)} \longleftrightarrow H_g(s) = \frac{1}{\phi^+(s)} \left[\text{causal} \left(\frac{P(-s)\, e^{-sT}}{\phi^-(s)} + C \frac{sP(-s)\, e^{-sT}}{\phi^-(s)} \right) \right]. \tag{2a}$$

The constant C is so selected that

$$h_g(\cdot) * p(\cdot) \Big|_{t=T} = 0. \tag{2b}$$

Numerous simulations pertinent to the Loran C environment have been performed. This work will continue.

T. L. Rhyne

B. RECONSTRUCTION OF TWO-DIMENSIONAL SIGNALS FROM PROJECTIONS

An ordinary x-ray represents a flat two-dimensional projection of the optical density of a three-dimensional object. If several of these projections are available from different directions, then the three-dimensional structure of an object can be obtained or approximated. Similarly, a two-dimensional signal can be approximated from several of its one-dimensional projections. Several techniques have been explored, some of which perform reconstructions in the frequency domain,[1-3] and some of which perform it in the time domain.[4] In this report we shall consider several of these reconstruction schemes from the point of view of digital signal processing, consider the relationship between a multidimensional signal and its projections, and report on the progress that has been made in this study. Specifically, we hope to answer questions such as: What restrictions must be imposed upon a multidimensional signal so that the reconstruction can be performed exactly? When the result of the reconstruction is an approximation, how well does the reconstruction reproduce the original signal?

If a projection p(x) is taken in the y direction on the function f(x, y), then

$$p(x) = \int_{-\infty}^{\infty} f(x, y)\, dy. \tag{1}$$

Furthermore, if F(X, Y) represents the Fourier transform of f(x, y)

$$F(X, Y) = \int_{-\infty}^{\infty} \int_{-\infty}^{\infty} f(x, y)\, e^{-j2\pi(xX+yY)}\, dxdy, \tag{2}$$

then

$$F(X, 0) = \int_{-\infty}^{\infty} \int_{-\infty}^{\infty} f(x, y)\, e^{-j2\pi xX}\, dxdy$$

$$= \int_{-\infty}^{\infty} e^{-j2\pi xX} \left[\int_{-\infty}^{\infty} f(x, y)\, dy \right] dx$$

$$= \int_{-\infty}^{\infty} e^{-j2\pi xX}\, p(x)\, dx. \qquad (3)$$

The one-dimensional Fourier transform of this projection, then, is numerically equal to the two-dimensional transform F(X, Y) evaluated along the line Y = 0.

It can be shown that if f(x, y) is represented in polar coordinates as $\overline{f}(r, \phi)$ and if F(X, Y) is represented as $\overline{F}(R, \theta)$, then $\overline{f}(r, \phi+\phi_o)$ transforms to $\overline{F}(R, \theta+\phi_o)$; that is, a rotation in the image plane corresponds to a rotation in the Fourier plane. Utilizing this fact and Eq. 3, we can obtain the Fourier transform F(X, Y) along the lines indicated in Fig. XII-1, by taking the one-dimensional Fourier transforms of 8 projections of f(x, y) at angles 0, $\pi/8$, $\pi/4$, $3\pi/8$, $\pi/2$, $5\pi/8$, $3\pi/4$, and $7\pi/8$.

One procedure for reconstructing f(x, y) from its projections would be, first, to Fourier-transform the projections. This will specify F(X, Y) along some lines in the

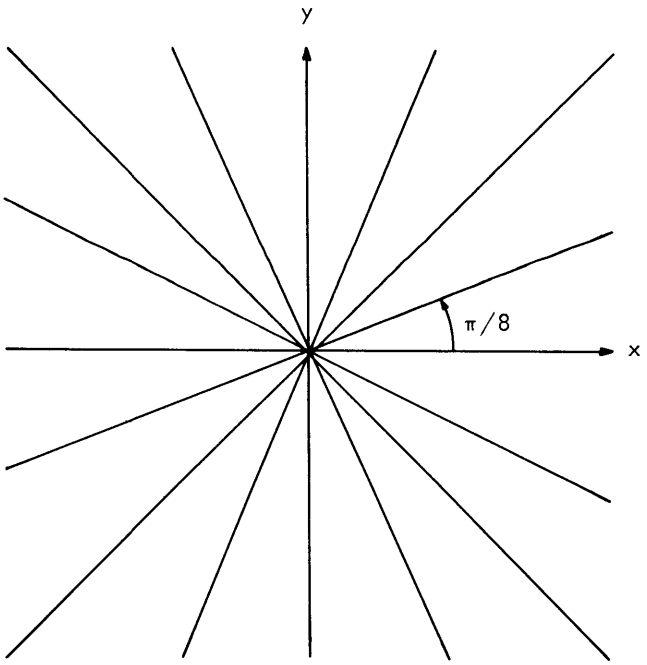

Fig. XII-1. Lines in the Fourier plane where F(X, Y) is known from equiangularly spaced projections.

Fourier plane. Then, subject to some assumptions about F(X, Y) (or f(x, y)), we can fill in the rest of the Fourier plane and generate an approximation $\hat{F}(X, Y)$ to F(X, Y). Finally, we can get our reconstruction $\hat{f}(x, y)$ by letting

$$\hat{f}(x, y) = \int_{-\infty}^{\infty} \int_{-\infty}^{\infty} \hat{F}(X, Y)\, e^{j2\pi(xX+yY)}\, dXdY. \tag{4}$$

The accuracy of the reconstruction will depend upon the number of projections, the assumptions made in filling in the Fourier plane and inherent errors, such as inaccurate projections and inaccuracies in performing the integrations.

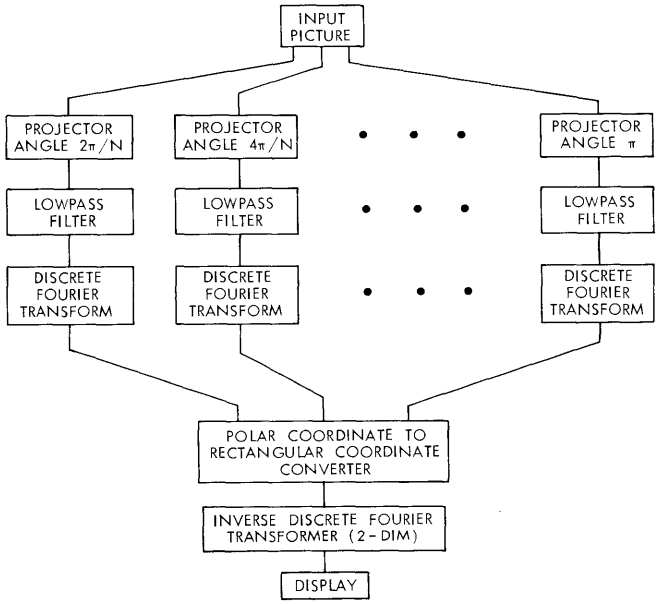

Fig. XII-2. A system used to implement the reconstruction.

The system that is block-diagrammed in Fig. XII-2 was used to implement the reconstruction. The projections were computed, lowpass-filtered (to remove noise generated in the computation), and transformed. At this stage, F(X, Y) was known at points on a regular polar raster (points equally spaced in radius and angle). Interpolation was then used to approximate F(X, Y) at points on a regular Cartesian raster, after which an inverse two-dimensional discrete Fourier transform was computed. The interpolation at this stage of the work was simple. The value of $\hat{F}(X, Y)$ at each Cartesian point was made equal to $\hat{F}(X, Y)$ at the nearest polar point (the nearest point computable from the projections). Other more accurate interpolation schemes will be tried later. Results of this technique are shown in Fig. XII-3 for pictures of different sizes. In Fig. XII-4

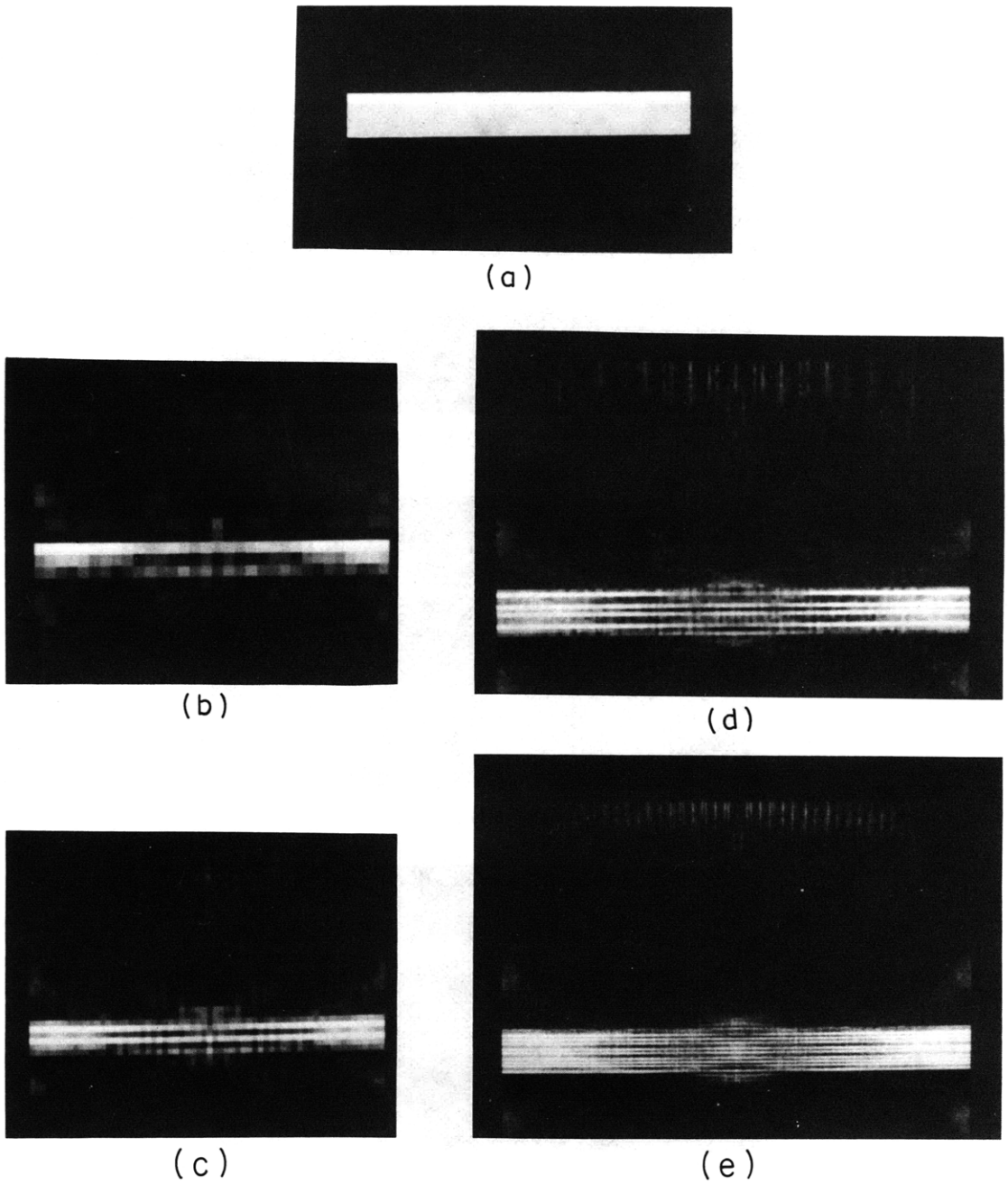

Fig. XII-3. Reconstructions by interpolating in the Fourier plane for pictures of different sizes.
(a) original picture.
(b) 32 × 32 picture.
(c) 64 × 64 picture.
(d) 128 × 128 picture.
(e) 256 × 256 picture.

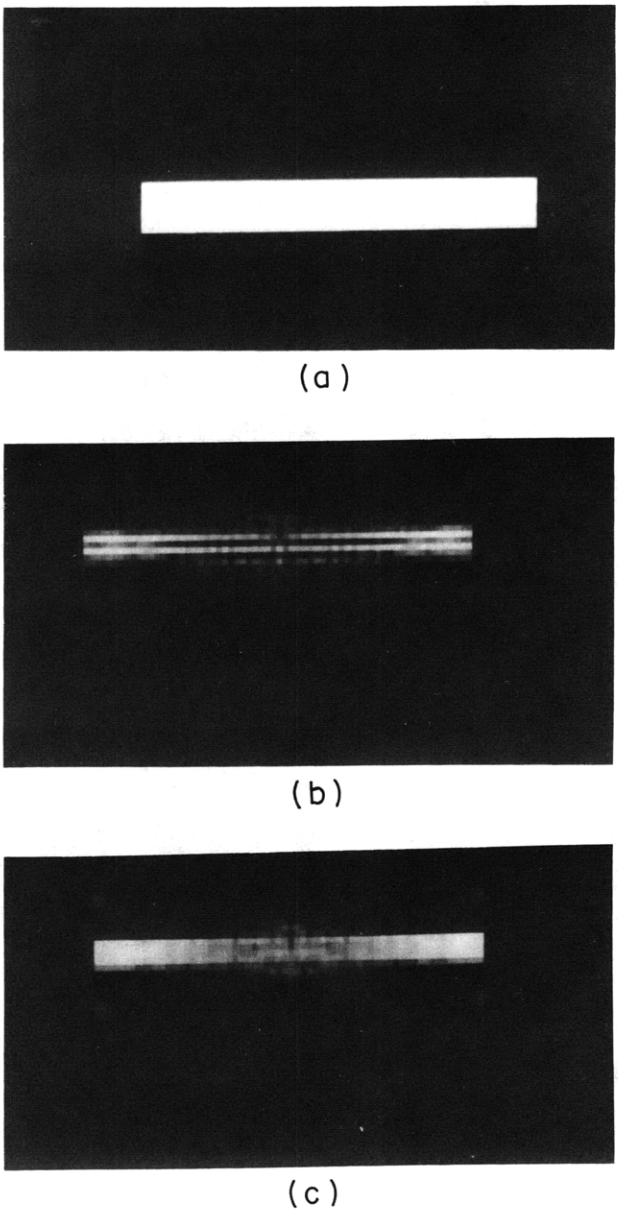

Fig. XII-4. (a) Original function (64×64).
(b) Reconstruction with unfiltered projections.
(c) Reconstruction with filtered projections.

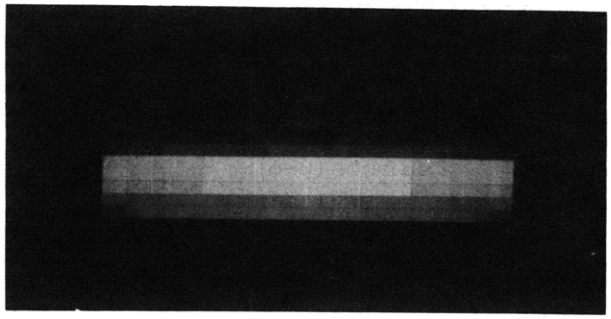

(a)

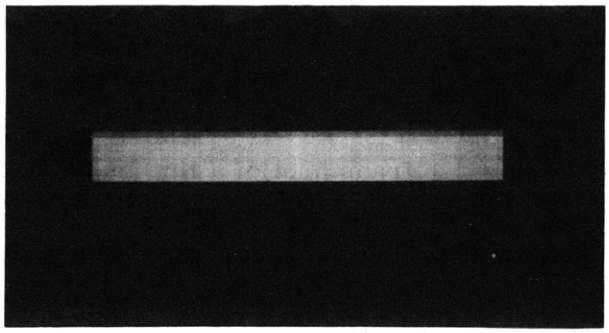

(b)

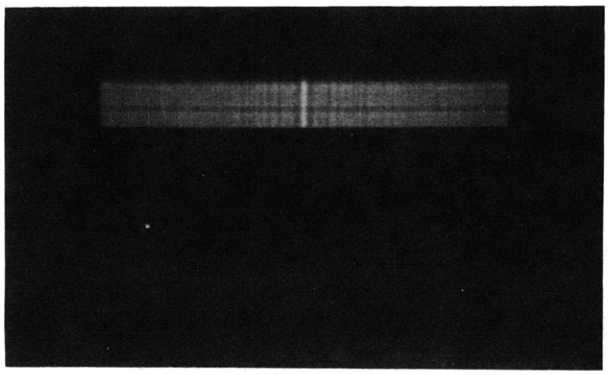

(c)

Fig. XII-5. Results of a reconstruction implemented by the procedure of Eq. 6.
(a) 32 × 32 picture.
(b) 64 × 64 picture.
(c) 128 × 128 picture.

reconstructions whose projections were lowpass-filtered are compared with reconstructions whose projections were unfiltered.

Another approach that has been tried is to write the inverse transform in polar coordinates,

$$f(r,\phi) = \int_0^{\infty} \int_{-\pi}^{\pi} F(R,\theta)\, e^{j2\pi Rr\cos(\theta-\phi)}\, R\,d\theta\, dR. \tag{5}$$

Since we know $F(R,\theta)$ along lines $\theta = \theta_i$ for several values of i, we can approximate the integral by a sum.

$$\hat{f}(r,\phi) = \frac{\pi}{N} \sum_{i=0}^{N-1} F(R,\theta_i)\, R\, e^{j2\pi Rr\cos(\theta_i-\phi)}\, dR. \tag{6}$$

The integral is simply the inverse transform of a line impulse and so must be constant along a line perpendicular to the line $\phi = \theta_i$. Parallel to this line it simply represents a modified projection function (the modification is due to the factor of R which multiplies $F(R,\theta)$). Hence these can be called modified smeared projections. This reconstruction procedure informs us that $f(x,y)$ is approximately the sum of the modified smeared projections of $f(x,y)$. Some results obtained from this procedure are shown in Fig. XII-5.

R. M. Mersereau

References

1. R. A. Crowther, D. J. DeRosier, and A. Klug, "The Reconstruction of a Three-Dimensional Structure from Projections and Its Application to Electron Microscopy," Proc. Roy. Soc. (London) A 317, 319-340 (1970).
2. D. J. DeRosier and A. Klug, "Reconstruction of Three-Dimensional Structures from Electron Micrographs," Nature 217, 130-134 (1968).
3. J. B. Garrison, D. G. Grant, W. H. Guier, and R. J. Johns, "Three-Dimensional Roentgenographs," Am. J. Roentgenol., Radium Therapy, Nucl. Med. 60, 903-908 (1969).
4. R. Gordon, R. Bender, and G. T. Herman, "Algebraic Reconstruction Techniques for Three-Dimensional Electron Microscopy and X-ray Photographs," J. Theoret. Biol. 29, 471-481 (1970).
5. J. W. Klovstad, "Object Reconstruction from Shadow Images," S.M. Thesis, Department of Electrical Engineering, M.I.T., 1970.